An Investigation into the Dissipative Stochastic Mechanics Based Neuron Model under input Current Pulses

Mohamed N. Abdulmonim

Submitted to the
Institute of Graduate Studies and Research
in partial fulfillment of the requirements for the Degree of

Master of Science
in
Computer Engineering

Eastern Mediterranean University
April 2013
Gazimağusa, North Cyprus

Approval of the Institute of Graduate Studies and Research

Prof. Dr. Elvan Yılmaz
Director

I certify that this thesis satisfies the requirements as a thesis for the degree of Master of Science in Computer Engineering.

Assoc. Prof. Dr. Muhammed Salamah
Chair, Department of Computer Engineering

We certify that we have read this thesis and that in our opinion it is fully adequate in scope and quality as a thesis for the degree of Master of Science in Computer Engineering.

Prof. Dr. Marifi Güler
Supervisor

Examining Committee

1. Prof. Dr. Erden Başar

2. Prof. Dr. Marifi Güler

3. Asst. Prof. Dr. Ahmet Ünveren

ABSTRACT

It has been recently argued and experimentally shown that ion channel noise in neurons can have profound effects on the neuron's dynamical behavior. Most profoundly, ion channel noise was seen to be able to cause spontaneous firing and stochastic resonance.

A physical approach for the description of neuronal dynamics under the influence of ion channel noise has been proposed through the use of dissipative stochastic mechanics by Güler in a series of papers (Güler, 2006, 2007, 2008). He consequently introduced a computational neuron model incorporating channel noise for a special membrane that gives the Rose-Hindmarsh model of the neuron in the deterministic limit. The most distinctive feature of the dissipative stochastic mechanics based model is the presence of so-called the renormalization terms therein. More recently, the model was generalized to the Hodgkin-Huxley type of membranes (Güler, 2011, 2013).

In this thesis, the dissipative stochastic mechanics based neuron model was studied when the input current to the neuron is an input pulse. Statistics of firing efficiency, latency, and jitter were examined for various stimulus pulses. In particular, the role played by the presence of the renormalization terms was focused on in the examination.

Keywords: Ion Channel Noise, Stochastic Ion Channels, Neuronal Dynamic, Rose-Hindmarsh Model.

ÖZ

Gerek deneysel, gerekse kuramsal ve benzeşim çalışmaları iyon kanal gürültüsünün nöron dinamiği üzerinde hayati etki yapabildiği kanıtlanmıştır. Bu kapsamda, kendi kendine ateşleme ve stokastik rezonans en önemli bulgulardır.

İyon kanal gürültüsü altındaki nöron dinamiği, fiziksel bir yaklaşım olan disipatif stokastik mekanik kullanarak çalışılmış ve modellenmiştir (Güler, 2006, 2007, 2008). Sonsuz zar büyüklüğü limitinde Rose-Hindmarsh modeline dönüşen bu disipatif stokastik mekaniğe dayalı modelin en önemli özelliği renormalizasyon terimleri içermesidir. Model, daha sonra, Hodgkin-Huxley tipi zarlara uyarlanmıştır (Güler, 2011, 2013).

Bu tezde, Rose-Hindmarsh tipi zarlarda iyon kanal gürültüsü için geliştirilmiş olan yukarıdaki model, basamaklı girdi akımları kullanılarak çalışılmıştır. Ateşleme etkinliği, gecikme ve jitter istatistikleri elde edilmiş ve renormalizasyon terimlerinin rolü incelenmiştir.

Anahtar Kelimeler: İyon kanal gürültüsü, Stokastik iyon kanalları, Nöronal Dinamik, Rose-Hindmarsh Modeli.

I lovingly dedicate this thesis

TO MY BELOVED

Father & Mother

Uncles & Aunts

my brother

And all my friends

ACKNOWLEDGMENT

I would like to acknowledge with gratitude Prof. Dr. Marifi GÜLER, without his knowledge, guidance, supervising, and effort this research will be impossible.

TABLE OF CONTENTS

LIST OF FIGURES

Chapter 1

INTRODUCTION

Electrical variability is a prominent feature of neurons behavior which is known to be stochastic in nature (Fasial 2008). The main source of stochasticity is the external noise from the synaptic. Nevertheless, led by the present of the probabilistic character of gating ,the ion channel causes the intrinsic noise to appear which can also have an important effect on the dynamic behavior of neurons; as viewed by empirical studies (Bezrukov and Vodyanoy 1995; Sakmann and Neher 1995; Diba et al. 2004; Kole et al. 2006; Jacobson et al. 2005)and by numerical simulation or theoretical investigations (Chow and White 1996; Fox and Lu 1994; Schmid et al. 2001; Schneidman et al. 1998; Jung and Shuai 2001; Rubinstein 1995).

The effect of channel variability on neuronal dynamic is normally modeled using stochastic various equations obtained by introducing some white noise of vanishing means into underling deterministic equations (Fox and Lu 1994). The so-called dissipative stochastic mechanics ("DSM") based neuron model which was raised by Güler (2006, 2007) is a special situation to this. The DSM neuron model rise some functional terms named the renormalization term. The renormalization of the membrane capacitance and the membrane voltage dependent potential function were found to rise from the mutual interaction of the two noises in the neurons (Güler 2008). It was found

that the renormalization correction increases the behavioral transitions from quiet to spike and from tonic to bursting. The renormalization terms of neuronal dynamic can enhance temporal synchronization among synoptically coupled neurons which can lead to faster temporal synchronization (Jibril and Güler 2009) . In this thesis , we investigate the DSM model under input current pulses; especially, we concentrate on what role the renormalization terms can play in the statistics of efficiency, latency and jitter.

1.1 Scope and Organization

In this thesis, the DSM model, introduced by Güler (2007), will be examined, when the input current pulse varies. The organization of the thesis will be as follow, Chapter two handles neuron morphology and structure, chapter three focuses on the Hodgkin Huxley equation, Hind marsh and the DSM model. Chapter four is about the experiments and results of the study.

Chapter 2

NEURONS

2.1 Morphology and Structure

Neurons are a specialized type of cells found in the brain. They are unique in generating electrical signals in response to chemical and other inputs. A typical neuron is divided into three parts: the soma or cell body, dendrites, and axon. Dendrites receive inputs from other neurons cell and propagate it to the soma. The axon transmits the neuronal output to other cells. The dendrites tree increases surface area of the cell through the branching structure which improves the ability of the neuron to receive input from many other cells through synapses connections. Figure 1 depicts information and structure for the neuron. Axons from single neurons can traverse large fractions of the brain or, in some cases, of the entire body. It has been estimated that cortical neurons typically send about 40 mm of axon and have approximately 4 mm of total dendritic cable in their structural dendritic trees. The axon makes an average of 180 synaptic connections with other neurons per mm of length while the dendritic tree receives, on average, 2 synaptic inputs per μm. The cell body or soma of a typical cortical neurons ranges in diameter from about 10 to 50 μm (Abbot, 2002).

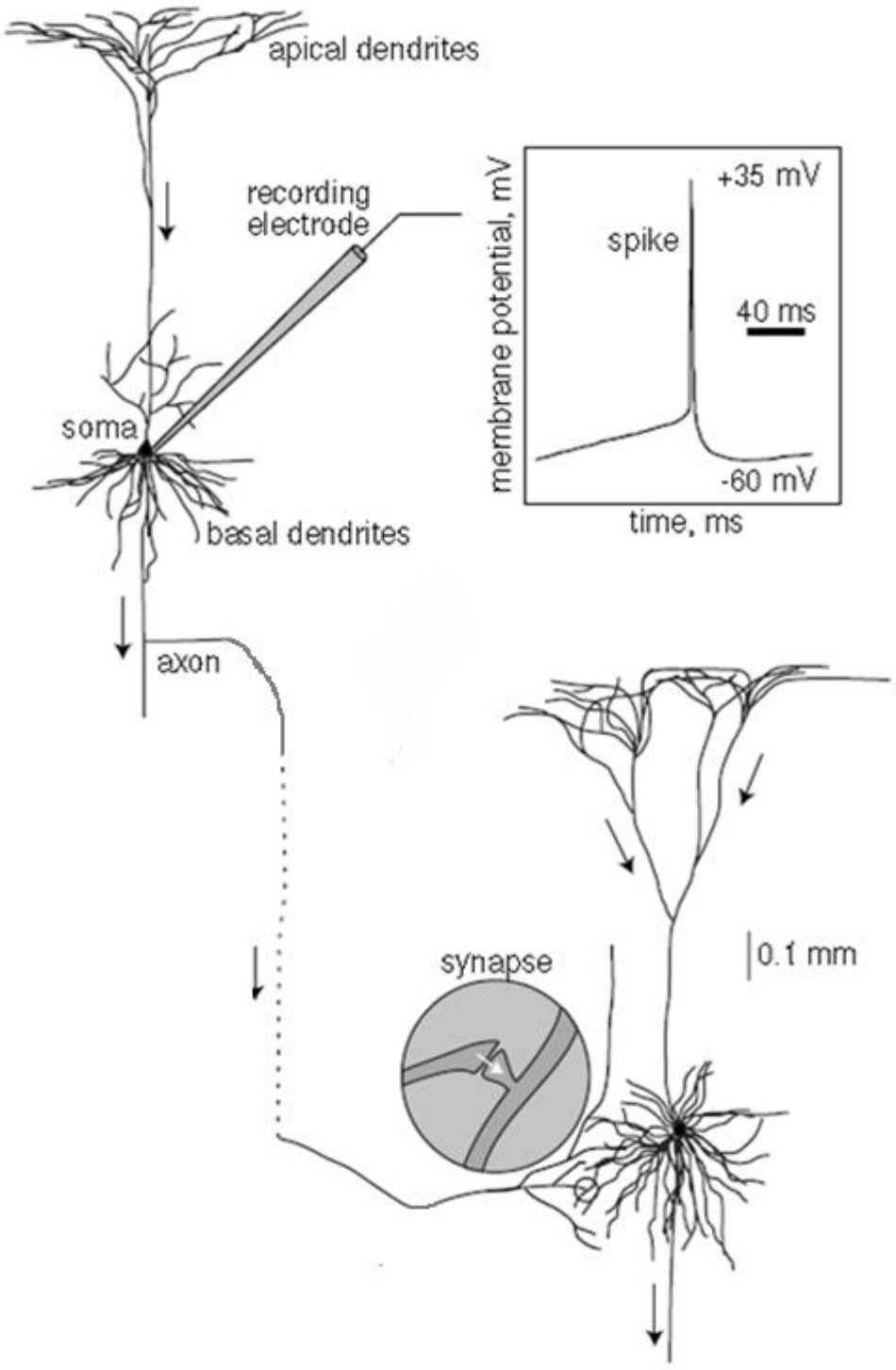

Figure 1: Two interconnected cortical pyramidal neurons (and in vitro recorded spike). (Izhikevich, 2007)

2.1.1 What is a Spike?

The communication mean between the neurons in simply a current pulse is known as a Spike. Neurons normally receive 10,000 ---from another through the synapse. On the other neuron when the signal is received ,this signal causes changes in the current of the transmembrane. The current coming from the synapse is known as the post synapse potentials (PSPs), little PSPs are generated from tiny current, large PSPs are generated when the current is considerably high. The voltage sensitive channel is embedded in a neuron, these channels are resulting to generation of action potential or spike (Izhikevich, 2007).

2.1.2 Membrane Proteins

Protein is an integral part of the cell membrane that transports molecules across it. These proteins play a significant part in determining the function of neurons. Knowing how membrane proteins work is useful for understanding many functions of neurons. We describe many categories of membrane proteins that assist in transporting substances across the membrane like channels, gates, and pumps.

2.1.2.1 Channels

Some membrane proteins are shaped in such a method that the create channels, or holes, across that substances can pass. Disparate proteins with different-sized holes permit disparate substances to go in or depart the cell. Protein molecules assist as channels for predominantly sodium (Na^+), potassium (K^+), calcium (Ca^{2+}), and chloride (Cl^-) ions.

2.1.2.2 Gates

A vital feature of a little protein molecules is their skill to change shape. some gates work by changing form after one more chemical binds to them. In these cases, the embedded protein molecule deeds as a door lock. After a key of the appropriate size and

form is inserted into it and turned, the locking device adjusts the form and becomes activated. Other gates change form when certain conditions in their environment, such as electrical or temperature, change.

2.1.2.3 Pump

In some cases, a membrane protein deeds as a pump, a transporter molecule that needs power to move substances across the membrane. For instance, there is a protein that adjusts its form to impel Na+ ions in one direction and K+ ions in the other direction. Countless substances are transported by protein pumps. Channels, gates, and pumps play an important role in a neuron's ability to convey information.

2.1.3 Synapse

Synapses are shaped in the form of a junction amid two consecutive neurons after the axon of afferent neuron is related to the efferent one and provides a method to communicate the data to other cell. Axons terminate at synapses whereas the voltage transient of the action potential opens ion channels producing an influx of Ca2+ that leads to the discharge of a neurotransmitter. The neurotransmitter binds to receptors at the gesture consenting or postsynaptic side of the synapse provoking ion-conducting channels to open. Reliant on the nature of the ion flow, the synapses can have an excitatory, depolarizing, or an inhibitory, normally hyperpolarizing, result on the postsynaptic neuron (Abbot 2002).

Synapses are not randomly distributed above the dendritic surface. In finish, inhibitory synapses are more proximal than excitatory synapses, even though they are additionally present at distal dendritic spans and, after being present, on some spines in conjunction

alongside an excitatory input (Segev in Bower and Beeman 2003). In countless systems (e.g., pyramidal hippocampal cells and cerebellar Purkinje cells), a given input basis is preferentially mapped onto a given span of the dendritic tree, rather being randomly distributed above the dendritic surface. Electron micrographic pictures of synapses in real neurons are shown in figure 2.

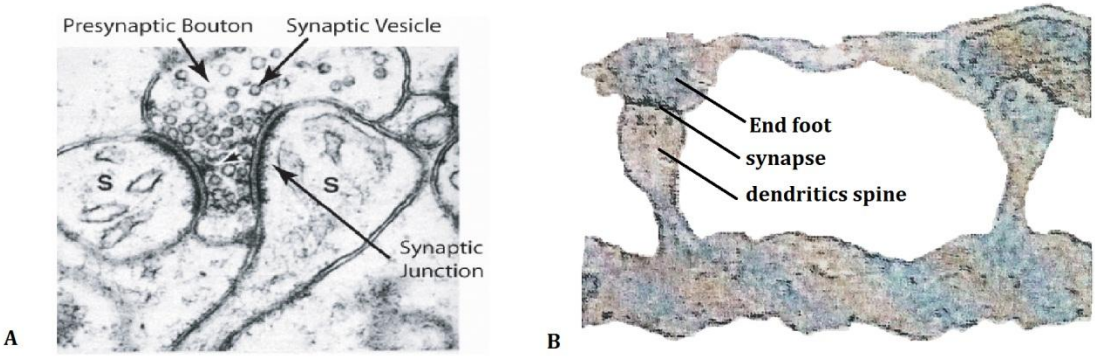

Figure 2: Two Electronic micrographic picture of synapse in real neurons

(a) Electron micrograph of recitative spiny synapses (s) designed on the dendrites of rodent hippocampal pyramidal cell

(b) An electron micrograph picture catches the synapse design where the terminal button of one neuron connects with a dendritic spine on a dendrite of second neuron. (Whishaw, 2012)

2.2 Membrane Potential and Neuron Electrical Activity

Membrane potential is defined as difference in electrical potential between the inside of a neuron and the surrounding extracellular fluid. Under resting conditions, the potential inside the cell membrane of a neuron is about -70 mV relative to that of the surrounding bath. This voltage, however, is conventionally assumed to be 0 mV for convenience and

the cell is said to be polarized in this state. This potential is an equilibrium point at which the flow of ions into the cell matches that out of the cell. This membrane potential difference is sustained by ion pumps located in the cell membrane by maintaining concentration gradients. For example, Na+ is much more concentrated outside a neuron than inside it, and the concentration of K+ is significantly higher inside the neuron than in the extracellular fluid. Therefore, ions flow into and out of a cell due to both voltage and concentration gradients throughout the state transition of cell. Current, in the form of positively charged ions flowing out of the cell (or negatively charged ions flowing into the cell) through open channels makes the membrane potential more negative, a process called hyperpolarization. Current flowing into the cell changes the membrane potential to less negative or even positive values. This is called depolarization. When a neuron is depolarized sufficiently large to raise the membrane potential above a threshold level, a positive feedback process is started, and the neuron generates an action potential. An action potential is a roughly 100 mV fluctuation in the electrical potential across the cell membrane that lasts for about 1ms. Once an action potential takes place it may be impossible to initiate another spike right after the previous one and this is called the absolute refractory period. The importance of action potential is that unlike subthreshold fluctuations that attenuate over distance of at most 1 millimeter they can propagate over large distances without attenuation along axon processes (Dayan and Abbot 2002). Figure 3 depicts the voltage dynamic of a neuron during an action potential while it is synthesized by corresponding ion channel activities throughout an action potential. In this figure the resting potential is in its real value -70 mV.

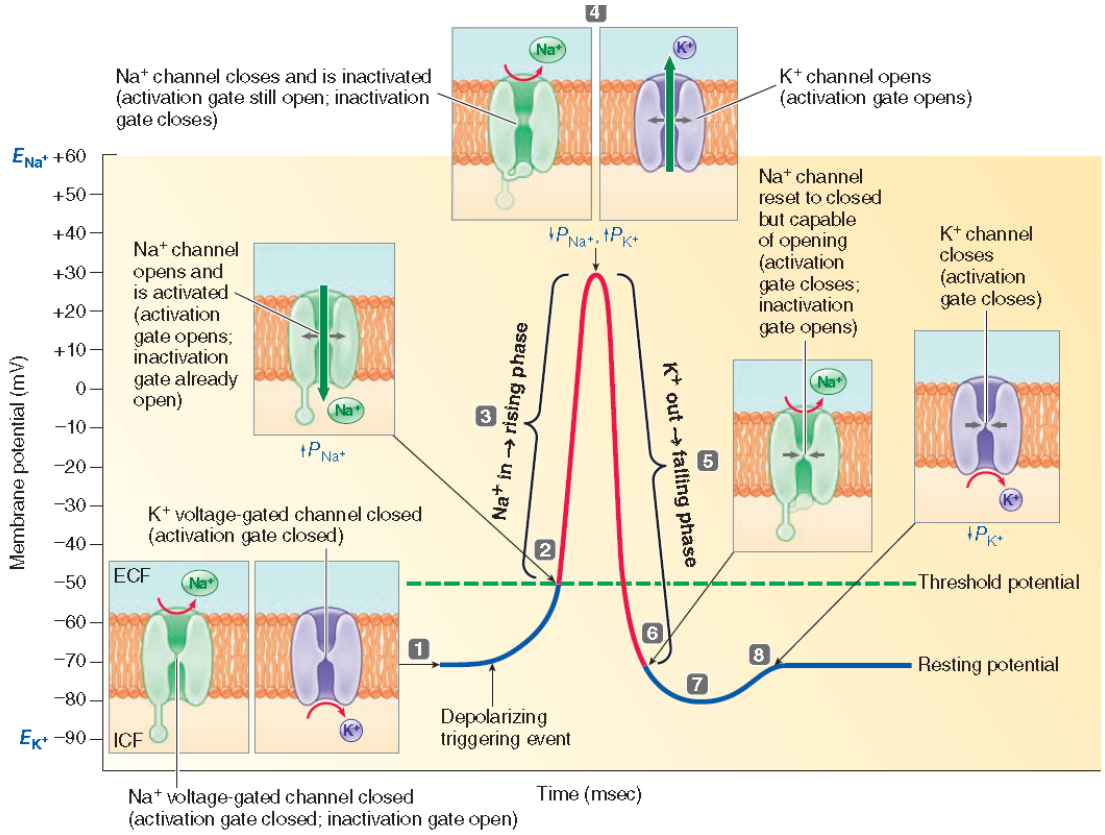

1. Resting potential: all voltage-gated channels closed.
2. At threshold, Na+ activation gate opens and P_{Na+} rises.
3. Na+ enters cell, causing explosive depolarization to +30 mV, which generates rising phase of action potential.
4. At peak of action potential, Na+ inactivation gate closes and P_{Na+} falls, ending net movement of Na+ into cell. At the same time, K+ activation gate opens and P_{K+} rises.
5. K+ leaves cell, causing its repolarization to resting potential, which generates falling phases of action potential.
6. On return to resting potential, Na+ activation gate closes and inactivation gate opens, resting channel to respond to another depolarizing triggering event.
7. Further outward movement of K+ through still-open K+ channel briefly hyperpolarizes
membrane, which generates after hyperpolarization.
8. K+ activation gate closes, and membrane returns to resting potential.

Figure 3: Phases of action potential (Whishaw, 2012)

Chapter 3

HODGKIN - HUXLEY EQUATIONS

Many neurons model have been found and developed in the last 6 decades, according to the purpose they used for. Furthermore, the diversity of the models found depends on the actual biophysical model with respect to structure. For instant, Hodgkin – Huxley (HH) during 5 decades is the more applicable model until now, also one of them is the simplified model used in the experiments of this thesis: the Hindmarsh-Rose model (HR). However, modeling technic of neural excitability has been attached from the monument work of Hodgkin-Huxley (1952). In this part , Hodgkin – Huxley model and the Hind marsh-Rose model (HR) will be briefly explained.

This chapter briefly handles both the Hodgkin-Huxley model and Hind marsh-Rose model (HR), followed by focusing on the latest physical inspiration of dissipative stochastic mechanics (DSM) established from the neuron model that achieves the deterministic condition of the dynamics of the HR model, and that will be focused and experimented in this study.

3.1 The Hodgkin-Huxley Model

According to Alan Lloyd Hodgkin and Andrew Huxley investigations, on giant squid axon in 1952, they found according to their experiments a way to describe the ionic mechanisms, initiation and propagation of spike. In their model based on experiments on

the squid axon membrane they show the current propagate through made from two significant ionic parts the first one I_{Na} (sodium channel current) and the second I_K (potassium current). Hodgkin and Huxley through their experiments found and developed a mathematical way leading to create the Hodgkin-Huxley model; the model found to be the mostly affective one based until our present time.

According to the model of Hodgkin – Huxley, they describe the electrical characteristics of membrane nerve patch, as an equivalent circuit. In this patch all the current across is made from two basic sections: charging membrane capacitance is the first one and the second is attached to transport a specific kind of ions via the membrane. Furthermore the ionic currents is made from three distinct ingredient, the sodium, the potassium and the chloride, (sodium current I_{Na}, potassium current I_K and leakage current I_L which is related to chloride).

According to Hodgkin-Huxley electrical circuit, the formula will be:

$$C_m \frac{dV_m}{dt} + I_{ion} = I_{ext} \quad (1)$$

Where

C_m is membrane capacitance

V_m is membrane potential

I_{ext} is an externally current

I_{ion} is the ionic current

The ions currents across the membrane could be found from the below equation as follow

$$I_{ion} = \sum_i I_i \quad (2)$$

$$I_i = g_i(V_m - E_i) \quad (3)$$

The currents in the equation (3) each one is related with a conductance g_i with reactive potential E_i

According to Hodgkin-Huxley the ionic currents that across the membrane in the Iion squid giant axon is actually three: I_{Na} (sodium current), I_K (potassium current) and a small leakage current I_L, as shown in the following equations.

$$I_{ion} = I_{Na} + I_K + I_L \quad (4)$$

$$I_{Na} = g_{Na}(V_m - E_{na}) \quad (5)$$

$$I_K = g_K\,(V_m - E_K) \quad (6)$$

$$I_L = g_L\,(V_m - E_L) \quad (7)$$

The conductance g_i (g_L, g_K, g_{Na}) are generated from the combined effect of a large amount of microscopic ion channels. The definition Iion is simply like the amount of open physical gates. These gates usually control the passage of ions through the channel. The ions can transport through the channel only when the channel is open, the channel is considered open only when the entire gates of that channel are in permissive state.

3.1.1 The Ionic Conductance

As mentioned earlier, in order to count the channel open, all the gates that belong to that channel must be in the permissive condition, through these channels the ions has the ability to pass through the membrane. The nominal assumption purposed to illustrate the potassium and sodium conductance is experimentally accomplished through voltage clamp experiments.

Where n, m and h are ion channel gate variables whose dynamics will be presented later on. $\bar{g}_{\text{i}}$ is representing the conductance constant for bounded area per cm^2(for remained the value of n as mentioned before is usually from 0 to 1). The dynamic of n, m, and h are as follows:

$$\dot{\text{n}} = \frac{dn}{dt} = \alpha_n(1-n) - \beta_n n \tag{8}$$

$$\dot{\text{m}} = \frac{dn}{dt} = \alpha_m(1-m) - \beta_m m \tag{9}$$

$$\dot{\text{h}} = \frac{dh}{dt} = \alpha_h(1-h) - \beta_h h \tag{10}$$

All of the rate constant (α_x and β_x) are voltage dependent which means that they are affected by the voltage changes, and they are independent with time, and n stands for the probability of the single gate to be in permissive state and it is a dimensionless variable. Usually the value of n is between 0 and 1.

The potential of membrane V_m (in voltage clamp test) starts usually from the resting period (V_m = 0) and followed by immediate arise to reach V_C. In order to find the solution to equation (9) above the following exponential can be used.

$$x(t) = x_\infty(V_c) - \big(x_\infty(V_c) - x_\infty(0)\big)\exp(-t/\tau_x) \quad (11)$$

$$x_\infty(0) = \alpha_x(0)/\alpha_x(0) + \beta_x(0) \quad (12)$$

$$x_\infty(V_c) = \alpha_x(V_c)/\alpha_x(V_c) + \beta_x(V_c) \quad (13)$$

$$\tau_x(V_c) = [\alpha_x(V_c) + \beta_x(V_c)]^{-1} \quad (14)$$

Here in these equations x stands for the time, which relies on all of the n, m and h (gate variable), as a consequence the formula becomes simpler, all of the values of the gate variable ($x_\infty(0) = 0$ at the resting state and $x_\infty(V_c) = V_c$). While τ_x here stands for the time needed to let x_∞ reach the steady state when the voltage of x_∞ reach V_c

The rate constant α_i β_i measured in H-H as function with V as follows:

$$\alpha_i = \frac{x_\infty(V)}{\tau_n(V)} \quad (15)$$

$$\beta_i = \frac{1 - x_\infty(V)}{\tau_n(V)} \quad (16)$$

As pointed before in the formulas, i is for n, m, and h. The below equations are for the rate constant α_i β_i, and could be determined from the following:

$$\alpha_n(V) = \frac{0.01(10 - V)}{\exp\left(\frac{10 - V}{10}\right) - 1}, \quad (17)$$

$$\beta_n(V) = 0.125 \exp\left(-\frac{V}{80}\right), \quad (18)$$

$$\alpha_m(V) = \frac{0.1(25 - V)}{\exp\left(\frac{10 - V}{10}\right) - 1}, \quad (19)$$

$$\beta_m(V) = 4 \exp\left(-\frac{V}{18}\right), \quad (20)$$

$$\alpha_h(V) = 0.07 \exp\left(-\frac{V}{20}\right), \quad (21)$$

$$\beta_h(V) = \frac{1}{\exp\left(\frac{30 - V}{10}\right) + 1} \quad (22)$$

All of α (V) and β (V) describe the transition rates between open and closed states of the channels.

3.2 The Hindmarsh Rose Model

Though Hodgkin-Huxley (HH) model can depict the neural dynamics of spiking neuron to a significant range, in large models the Hodgkin-Huxley (HH) bursting model can be complex. The axon of squid neuron had been studied by Hodgkin-Huxley who find out that it contains both Na and K conductance, while, there are more conductance kinds contribute in the HH bursting model which will increase the complexity in the model.

FitzHugh and Nagumo noticed separately in HH equations, that the developments in both membrane potential V(t) and sodium activation m(t) happened in similar time scales during an action potential, whereas the change in sodium inactivation h(t) as well as potassium activation n(t) are similar, although slower time scales. Consequently, the following equations can show the simulation of the model spiking behavior:

$$\dot{x} = a(y - f_1(x) + I), \quad \dot{y} = b(g_1(x) - y) \tag{23}$$

Where *x* stands for membrane potential and *y* denotes recovery variable. f_1(x) is a cubic function, $g_1(x)$ is a linear function, parameters a and b are time constants and $I(t)$ is the external applied or clamping current as function of time t.

Hindmarsh and Rose evolve their model by taking advantage of the FitzHugh-Nagumo model, which was a simplified version of the Hodgkin-Huxley equations and changed the linear function g(x) with a quadratic function so the model will be capable of rapid firing with a long interspace interval. Figure 4 demonstrates the 1982 Hindmarsh-Rose model null cline diagram.

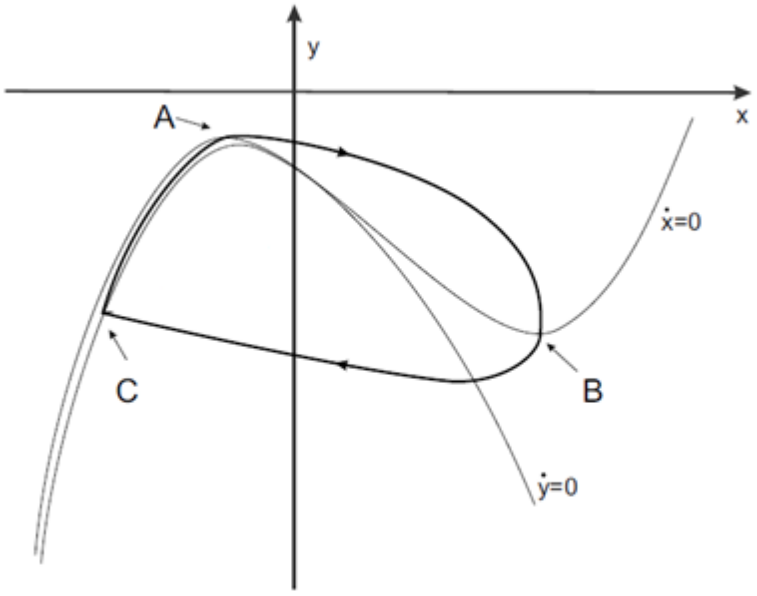

Figure 4: Analysis of the 1982 HR model phase plane. Null clines x= 0, y= 0 (thin lines) and firing limit-cycle (thick line). The model has one equilibrium point (Steur 2006).

In order to make the HR model exhibit burst firing behavior, more than one equilibrium point will be required; basically two points are required one for the sub-threshold stable resting state and one in the firing limit cycle. To make the null clines to intersect and bring about additive equilibrium points, a small deformation was required. The following forms were changes to meet the requirements of the governing equations:

$$\dot{x} = y - f(x) + I \, , \dot{y} = g(x) - y \qquad (24)$$

Where $f(x) = x^3 - 3x^2$ in the simple form of $f(x)$ in HR model, $g(x) = 1 - 5x^2$. The phase plane analysis of the given equations is shown in Figure 5.

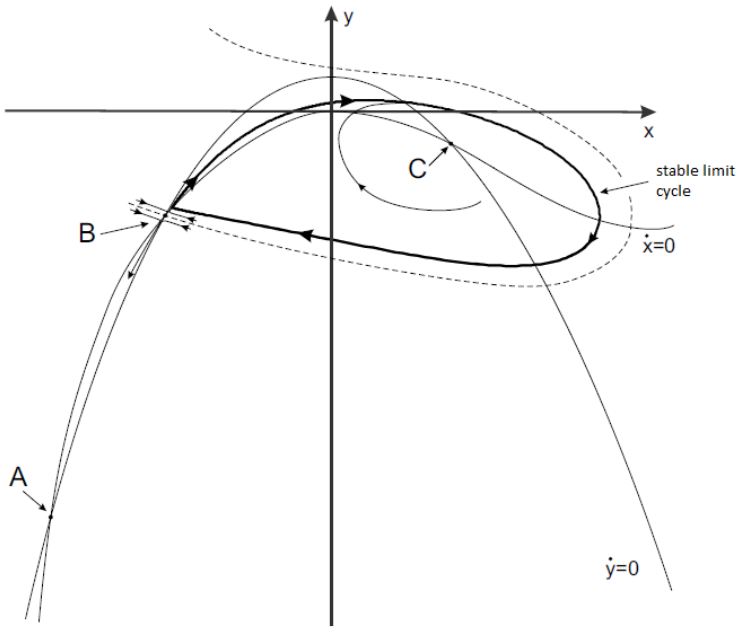

Figure 5: The representation of Rose Hindmarsh Model phase plane. The equilibrium points A, B and C is a stable node, an unstable saddle, and an unstable spiral, respectively. A simple form of f(x) is used in this equation as shown $\dot{\boldsymbol{x}} = \mathbf{0}$ nullcline (Steur 2006).

The corresponding point to the resting state of neuron is A in the diagram and it is a stable node. By using a large enough de-polarizing current pulse, the $\dot{x} = 0$ nulcline will be minimized such that the saddle point B and point A meet and eventually vanish. From this point, the state will increase the narrow channel and enter a stable limit cycle. But, ending the firing is impossible by simply terminating the stimulus and the state will leave the limit cycle by using a suitable hyper-polarizing pulse. So, to end the model firing state the term z was added to the model. This additive variable is a slowly varying current, the effective input I - z replaces the applied current I. When the neuron is in firing state the value of z should be increased. The general set of equations for HR model's after this improvement is as follows:

$$\dot{x} = -x^3 + 3x^2 + y + I - z \tag{25}$$

$$\dot{y} = 1 - 5x^2 - y$$

$$\dot{z} = r(h(x) - z)$$

Notice that the equivalents of both f(x) and g(x) have been added instead of them. In these equations x stands for membrane potential, y denotes recovery variable, and z is the adaptation current with time constant r. Variable z rises up during the firing state and decreases during the non-firing state. Parameters h and r made the model capable of showing bursting, chaotic bursting and post-inhibitory rebound. (Rose and Hindmarsh 1984; Steur 2006). Figure 6 shows the phase plane analysis of equation (25) using a complex form of f(x) as suggested in (Rose and Hindmarsh 1984).

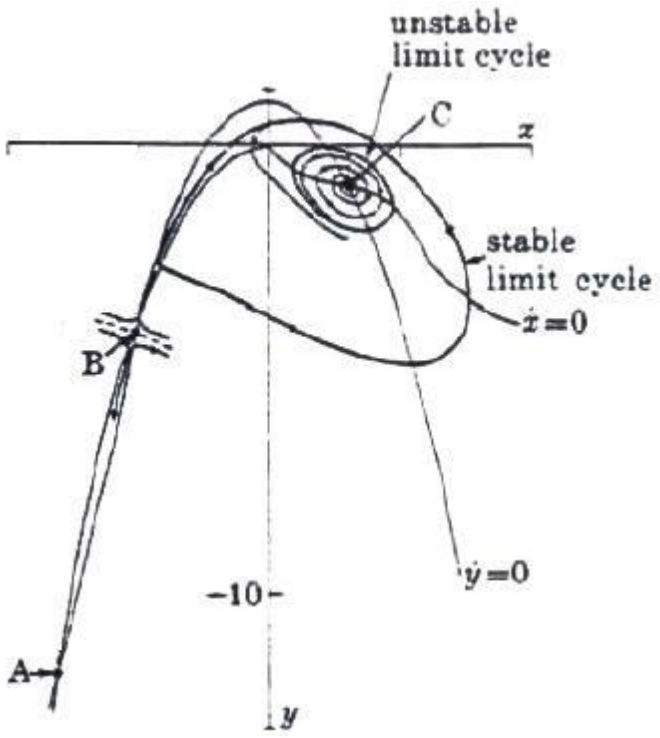

Figure 6: Phase plane representation of Rose Hind marsh Model using a complex form of f(x). The equilibrium points A, B and C is a stable node, an unstable saddle, and an unstable spiral, respectively. Unstable limit cycle is specified here (Rose and Hindmarsh 1984).

3.3 The DSM Neuron Model

The distinctive formulation of the Dissipative Stochastic Mechanics based (DSM) neuron stems from a viewpoint that conformational changes in ion channels are exposed to two different kinds of noise. These two kinds of noise were coined as the intrinsic noise and topological noise. The intrinsic noise arises from voltage dependent movement of gating particles between the inner and the outer faces of the membrane which is stochastic; therefore, gates open and close in a probabilistic fashion, that is, it is the average number, not the exact number, of open gates over the membrane which is specified by the voltage. The topological noise, on the other hand, stems from the presence of a multiple number of gates in the channels and is attributed to the fluctuations in the topology of open gates, rather than the fluctuations in the number of open gates.

Curiously, since gating particles, throughout the dynamics, do not follow a prescribed order in occupying the available closed gates, and in vacating the open gates, the membrane at two different times may have the same number of open gates but two different conductance values. The topological noise is attributed to the uncertainty in the number of open channels that takes place even if the number of open gates is exactly known. Hence, in determining the voltage dynamics, all the permissible topologies of open gates should be respected. Formalism of the DSM neuron was developed using the Rose Hindmarsh model (Hindmarsh and Rose 1984) and makes use of the Nelson's stochastic mechanics (Nelson 1966 and 1967), in the presence of dissipation, for modeling the effects of ion channel noise on voltage dynamics of the membrane. The

effect of the topological noise on the dynamics of the neuron becomes more significant in smaller membrane sizes. Therefore in too large neurons the DSM neuron behaves as the Hindmarsh-Rose model does.

The DSM neuron formalism yields the equations of motion for both first and second cumulants of the variables. The second cumulants, which describe the neuron's diffusive behavior, do not concern us in the current thesis. First cumulants evolve in accordance with the following dynamics:

$$m\dot{X} = \Pi + S_5 I \tag{26}$$

$$\dot{\Pi} = -\left(\frac{3a}{m}X^2 - \frac{2b}{m}X + S_0\right)(\Pi + S_5 I) - S_1 a X^3 + S_2 X^2 + S_6 X - S_3 X_{eq}(I) + S_1 I + S_7 - (1-r)[k\left(1 - \frac{\varepsilon_m^y}{m}\right)z + (1-k)\left(1 - \frac{\varepsilon_m^z}{m}\right)y \tag{27}$$

$$\dot{y} = -y - dX^2 + c + n^y \tag{28}$$

$$\dot{z} = -rz + rh(X - x_s) + n^z \tag{29}$$

$$\Pi(t_0) = y(t_0) - z(t_0) - a\left(X(t_0)\right)^3 + b\left(X(t_0)\right)^2 + (1 - S_5)I(t_0) \tag{30}$$

Where *X* denotes the expectation value of the membrane voltage, and Π corresponds to the expectation value of a momentum-like operator. The auxiliary variables *y* and *z* represent the fast and the slower ion dynamics, respectively. *I* denotes the external current injected into the neuron, and *m* denotes the membrane capacitance. The parameters *a*, *b*, *c*, *d*, *r*, *h*, and x_s are some constants parameters. *k* is a mixing coefficient given by *k = 1/(1+r)*. S are some constants as follows:

$$S_0 \coloneqq k + (1-k)r \tag{31}$$

$$S_1 \coloneqq S_0 - [k\frac{\varepsilon_m^y}{m} + (1-k)r\frac{\varepsilon_m^z}{m}] \tag{32}$$

$$S_2 \coloneqq k\left(1-\frac{\varepsilon_m^y}{m}\right)(b-d) + (1-k)\left(1-\frac{\varepsilon_m^z}{m}\right)(rb-d) \tag{33}$$

$$S_3 \coloneqq k\varepsilon_u^y + (1-k)\varepsilon_u^z \tag{34}$$

$$S_4 \coloneqq k\frac{\varepsilon_m^y}{m} + (1-k)\frac{\varepsilon_m^z}{m} \tag{35}$$

$$S_5 \coloneqq 1 - S_4 \tag{36}$$

$$S_6 \coloneqq S_3 - S_5 rh \tag{37}$$

$$S_7 \coloneqq (rhx_s + c)S_5 \tag{38}$$

Equation (29) specifies the value of Π at the initial time t_0 in terms of the initial values of the other dynamical variables *X*, *y* and *z*, and the current *I*. *Xeq(I)* obeys the equation

$$\mathfrak{a}X_{eq}^3 - (b-d)X_{eq}^2 + h\left(X_{eq} - x_s\right) - c - I = 0 \tag{39}$$

Where x_s is a constant. $\eta^y$and η^z in Equations. (27) and (28) are Gaussian white noises with zero means and mean squares are given by

$$< n^y(t)n^y(t') >= 2mT\delta(t-t') \tag{40}$$

And

$$< n^z(t)n^z(t') >= 2rmT\delta(t-t') \tag{41}$$

Where obtained by means of the classical fluctuation-dissipation theorem. T here is a temperature-like parameter. The terms with the *correction coefficients* $\varepsilon_m^y, \varepsilon_u^y, \varepsilon_m^z$ and ε_u^z that take place in the above equations are the renormalization terms.

When the noise terms (η^y, η^z) are not included and all the correction coefficients are set to zero, the DSM dynamics becomes equivalent to the Rose-hindmarsh dynamics. All the parameters of the model, including time, are in dimensionless units. The original membrane voltage time series for Hindmarsh-Rose original model is for some various constant input currents are shown in the figure 7. Dynamical states of the Rose–Hindmarsh model are quiescence, bursting (rhythmic with a high degree of periodicity, or chaotic), and tonic firing.

Güler (2008) showed that the role played by the intrinsic noise, becomes more significant in smaller size of the membranes (or, equivalently, fewer channels) in DSM Neuron. The intrinsic noise can cause spiking activity in otherwise quiet deterministic model and results in bursting in larger input current values. The dynamics of DSM Neuron in a relatively smaller size of membrane is displayed in figure 8. Note that renormalization corrections have been set to zero so that the result is observed regardless of the topological noise effect.

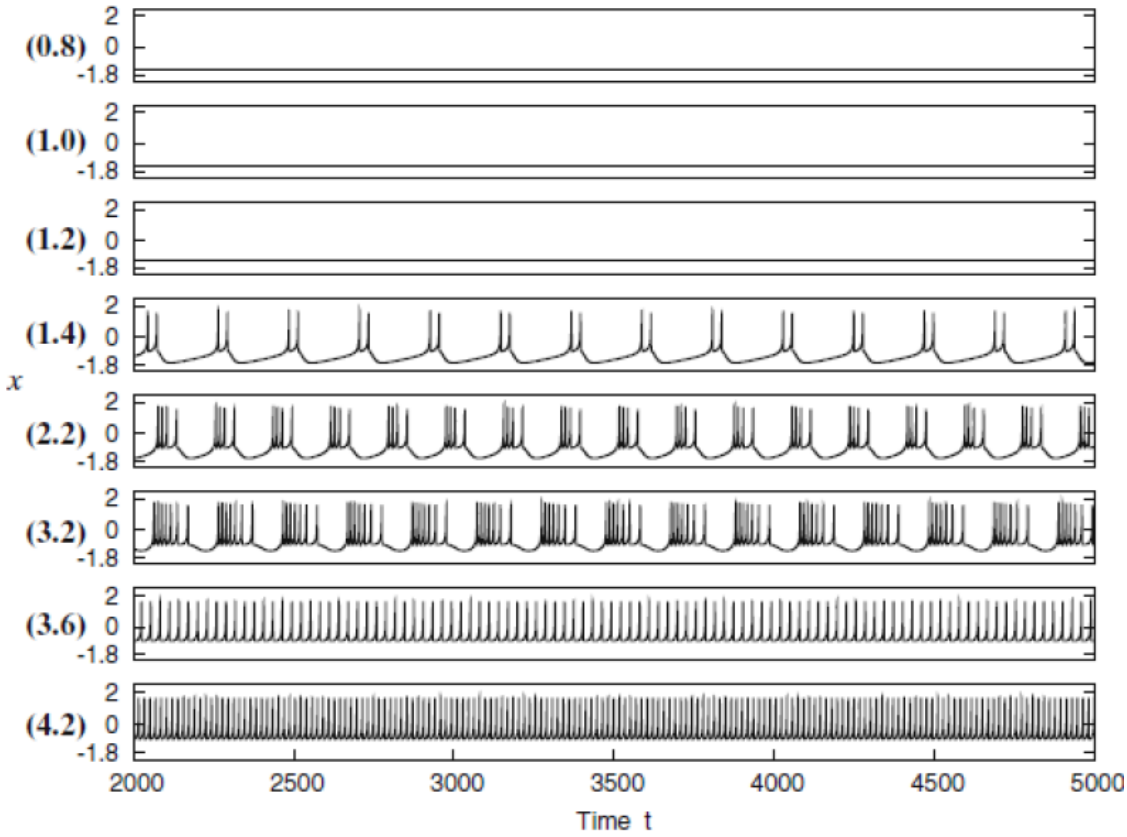

Figure 7: Membrane voltage time series of the deterministic Rose–Hindmarsh model using the parameter values m = 1, a = 1, b = 3, c = 1, d = 5, h = 4, r = 0.004 and x_s = −1.6; for various constant input current values I are indicated in parenthesis on the left of each plot (Güler 2008).

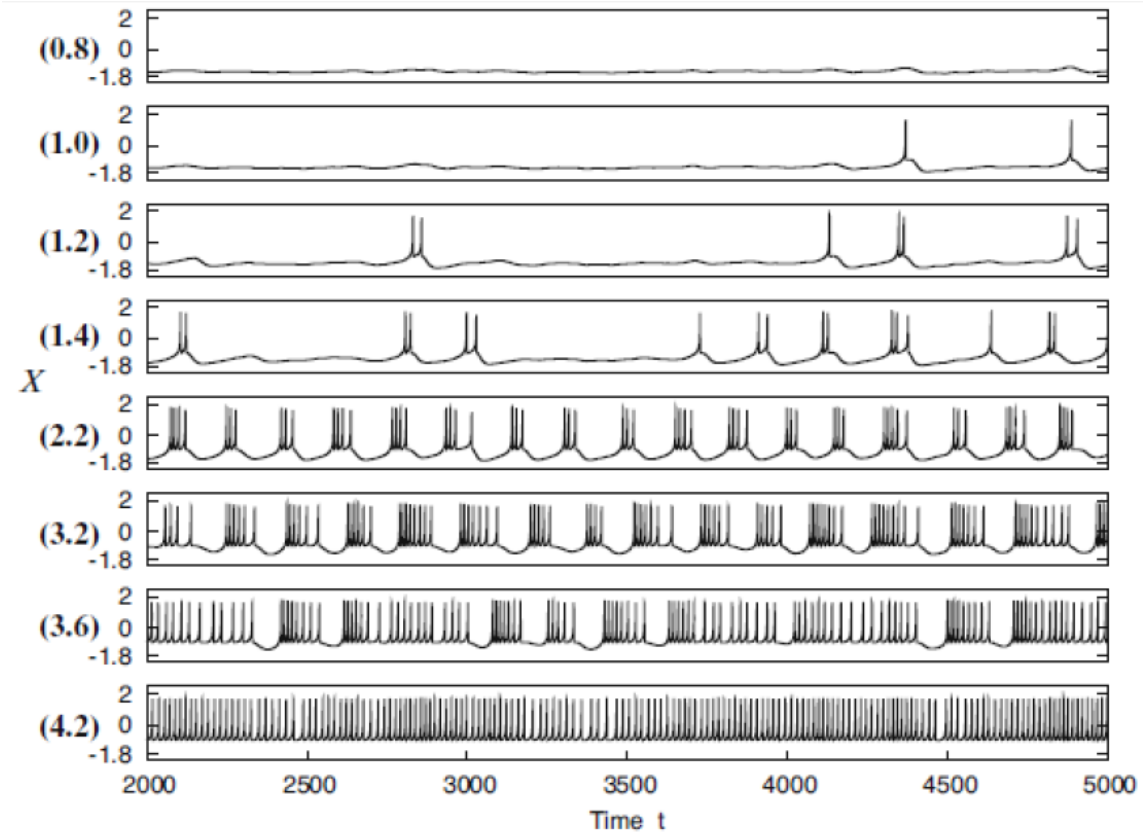

Figure 8: Time series of X when the DSM neuron is subjected to the intrinsic noise only using the Rose–Hindmarsh parameter values $m = 0.25$, $a = 0.25$, $b = 0.75$, $c = 0.25$, $d = 1.25$, $h = 1$, $r = 0.004$ and $x_s = -1.6$ with the temperature $T = 2$. Plots for various constant input current values $4I$ (scaled by the factor of four) (Güler 2008).

The renormalization corrections are induced by the mutual interaction between the topological noise and the intrinsic noise. Presence of the correction terms also increases further the behavioral transitions from quiescence to spiking and from tonic firing to bursting to a considerable extent and, consequently, leads to the bursting activity to take place in a wider range of input currents. i.e., with the presence of the correction terms, the spiking activity starts to take place at smaller input current values, and the bursting activity is prolonged for higher input current values. The behavior of DSM neuron under the influence of corrections is demonstrated in figure 9.

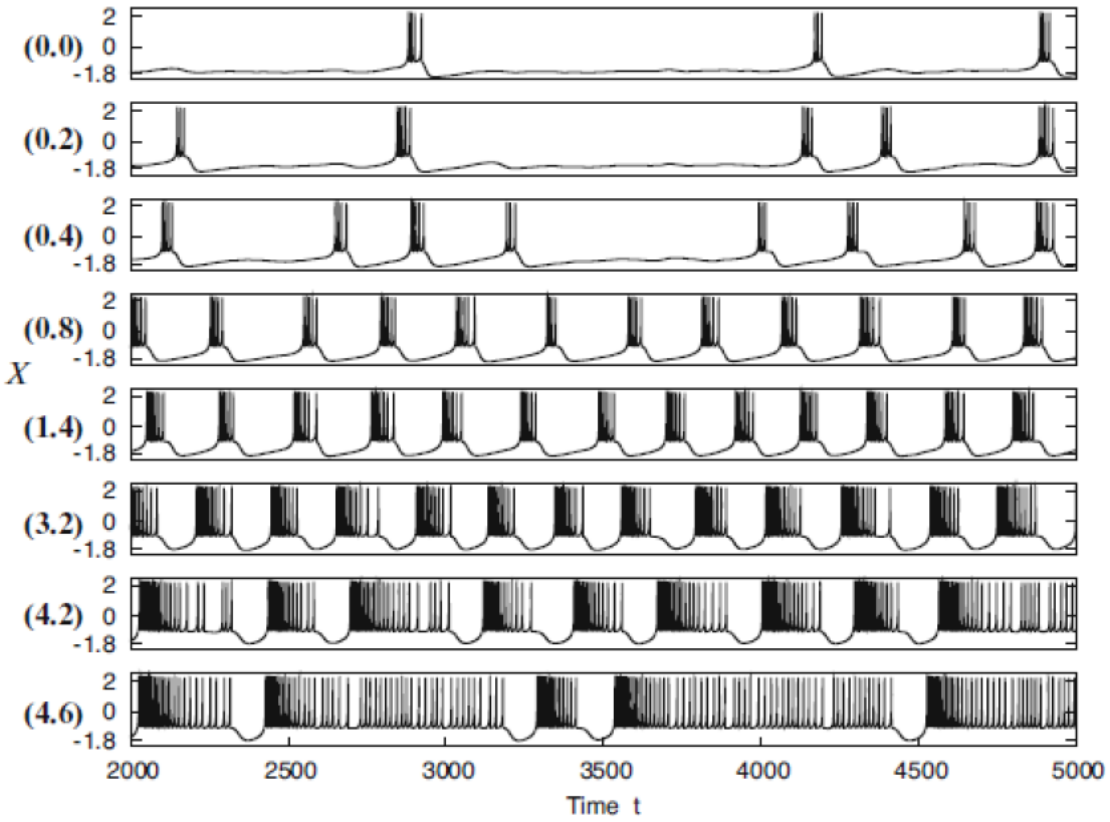

Figure 9: Time series of X using the correction coefficients $\varepsilon_m^y = 0.1, \varepsilon_u^y = 1.0, \varepsilon_m^z = 0.001$ and $\varepsilon_u^z = 0.005$ with the temperature T = 2. The Rose–Hindmarsh parameter values are m = 1, a = 1, b = 3, c = 1, d = 5, h = 4, r = 0.004 and $x_s = -1.6$ (Güler 2008).

Chapter 4

NUMERICAL EXPERIMENTS

4.1 The Role Played by the Renormalization Terms: Computing Efficiency, Jitter and Latency

We study the DSM model response to transient change in the stimulus. For this, we use a stimulus pulse as shown in figure 10.

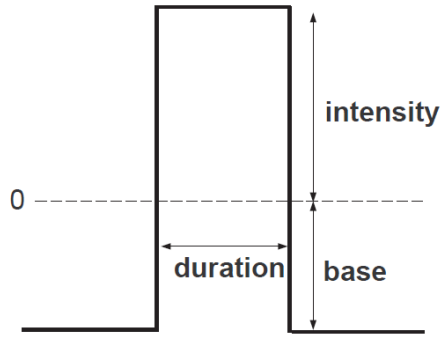

Figure 10: Wave form of the stimulus pulse used in this thesis. Various values of the pulse intensity were used in the experiments. The base current was set to two values 1in the first set and the other is 2 and the pulse duration to 100 ms.

Rather than investigating the role of the correction coefficients separately, we take the standard values of epsilons (renormalization terms) as follows ($\varepsilon_m^y = 0.1, \varepsilon_u^y = 0.5, \varepsilon_m^z = 0.001,$ and $\varepsilon_u^z = 0.005$) and scale them to zero to have a benchmark of various sets of correction coefficients, various values of the pulse intensity were used in the experiments. We use the following inputs for the neuron:

$$I = I_{base} + I_{intensity} \quad (42)$$

Where I_{base} indicates the base current and $I_{intensity}$current pulse intensity.

The model's behavior is studied in the context of efficiency, jitter and latency, here efficiency represented the fraction of trials which excite a spike; latency is the mean value of spike episode time with respect to the stimulation time; jitter is the standard deviation of the firing latency, within the following ranges of the parameters: I used intensity values between 0.5 and 4, I_{base} values is fixed to 1in the first set and 2 in the second set and the pulse duration is also fixed to 100 ms. Only the optimum result was taken in case of the lowest and highest spiking rate.

In the result of the experiments, the two curves representing the comparison between the renormalization terms when firstly the value of epsilon in set as the values ($\varepsilon_m^y = 0.1, \varepsilon_u^y = 0.5, \varepsilon_m^z = 0.001,$ and $\varepsilon_u^z = 0.005$) and secondly sets all the epsilons to zero. The experiments were done by changing the current pulse intensity and these methods (efficiency, latency, and jitter) are used to assess the effect of the renormalization terms as shown in the figures (11, 12, 13, 14, 15 and 16).

The effect of the renormalization terms appear in a significant manner when the value of the intensity is small but when the value of the intensity pass the value of (2) the impact of the renormalization terms almost vanish and the neuron reacts in the same way whatever the renormalization terms are exist or not as shown in figures (11, 12, and 13).

4.2 Technologies Used

The DSM neuron model has been developed by Prof. Marifi Güler and some parts have been changed in order to make it possible to do the experiments of this thesis. The model has been improved by the C++ language. The GnuPlot was used to plot the results and voltage time series.

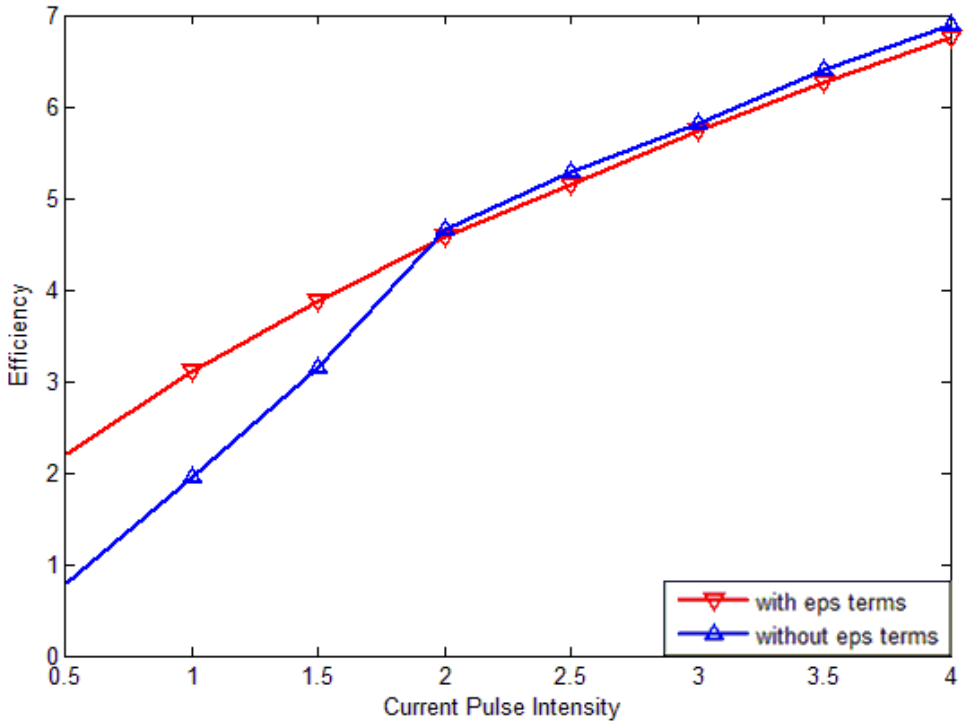

Figure 11: The difference in efficiency between the two experiments. In the first experiment epsilons value is set to $\varepsilon_m^y = 0.1, \varepsilon_u^y = 0.5, \varepsilon_m^z = 0.001$, and $\varepsilon_u^z = 0.005$ and the second experiment is set all the epsilons to 0. The intensity is shown in the figure and the I_{base} is set to 1.

In this figure, we got the result as shown above while using the renormalization terms (with eps terms) in the first experiments and second experiments the renormalization terms are set all to zero. We can see the effect of the renormalization in the beginning of the experiments.

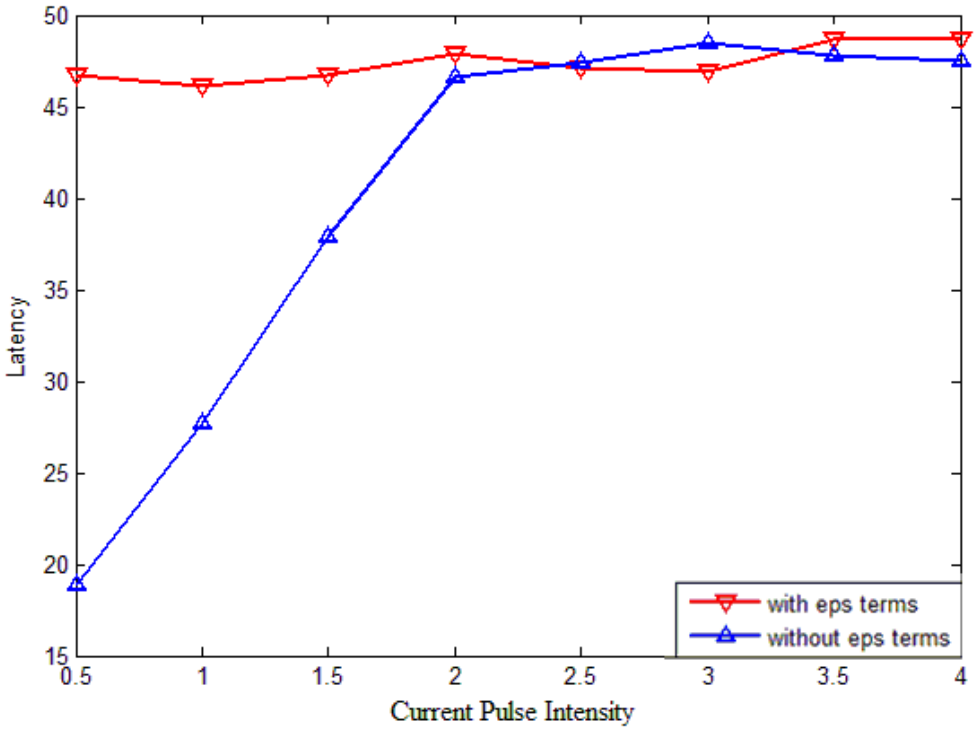

Figure 12: The difference in latency between the two experiments. In the first experiment epsilons value is set to $\varepsilon_m^y = 0.1$, $\varepsilon_u^y = 0.5$, $\varepsilon_m^z = 0.001$, and $\varepsilon_u^z = 0.005$ and the second experiment is set all the epsilons to 0. The intensity is shown in the figure and the I_{base} is set to 1.

In this figure, we got the result as shown above while using the renormalization terms (with eps terms) in the first experiments and second experiments the renormalization terms are set all to zero. We can see the effect of the renormalization in the beginning of the experiments.

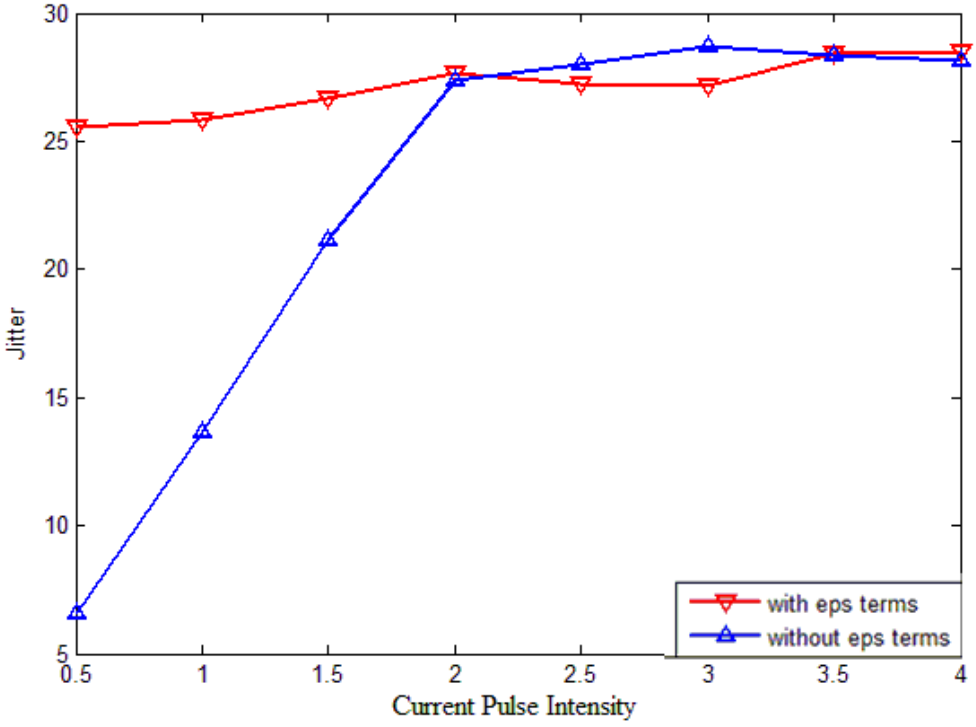

Figure 13: The difference in jitter between the two experiments. In the first experiment epsilons value is set to $\varepsilon_m^y = 0.1, \varepsilon_u^y = 0.5, \varepsilon_m^z = 0.001$, and $\varepsilon_u^z = 0.005$ and the second experiment is set all the epsilons to 0. The intensity is shown in the figure and the I_{base} is set to 1.

In this figure, we got the result as shown above while using the renormalization terms (with eps terms) in the first experiments and second experiments the renormalization terms are set all to zero. We can see the effect of the renormalization in the beginning of the experiments.

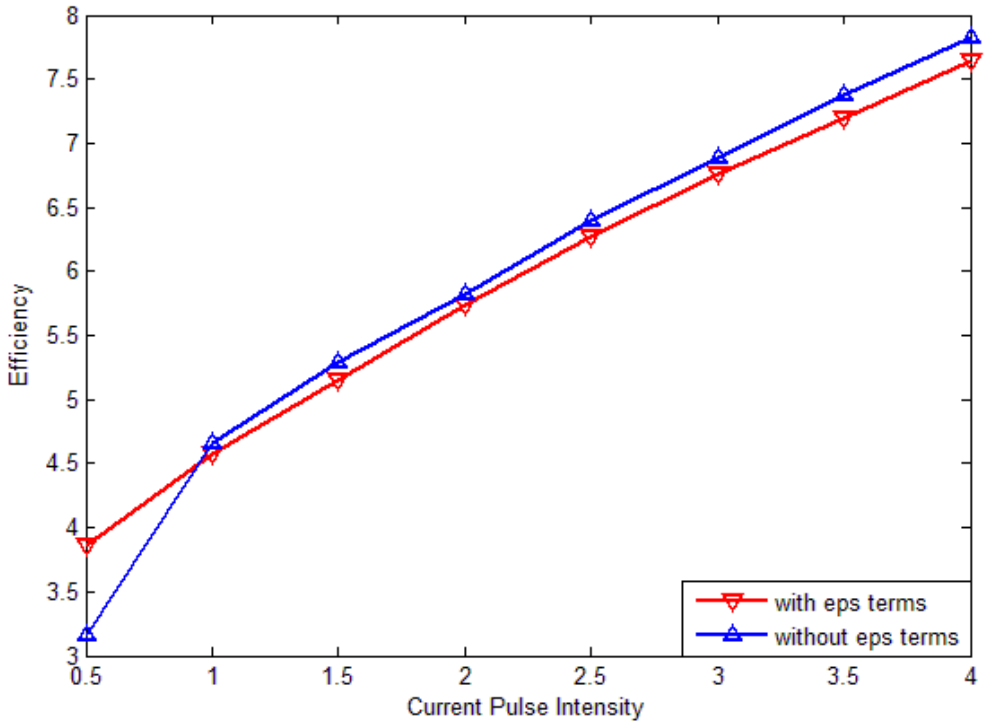

Figure 14: The difference in efficiency between the two experiments. In the first experiment epsilons value is set to $\varepsilon_m^y = 0.1, \varepsilon_u^y = 0.5, \varepsilon_m^z = 0.001$, and $\varepsilon_u^z = 0.005$ and the second experiment is set all the epsilons to 0. The intensity is shown in the figure and the I_{base} is set to 2.

In this figure, we got the result as shown above while using the renormalization terms (with eps terms) in the first experiments and second experiments the renormalization terms are set all to zero. We can see the effect of the renormalization in the beginning of the experiments become smaller than the effect in the figure (11,12,13).

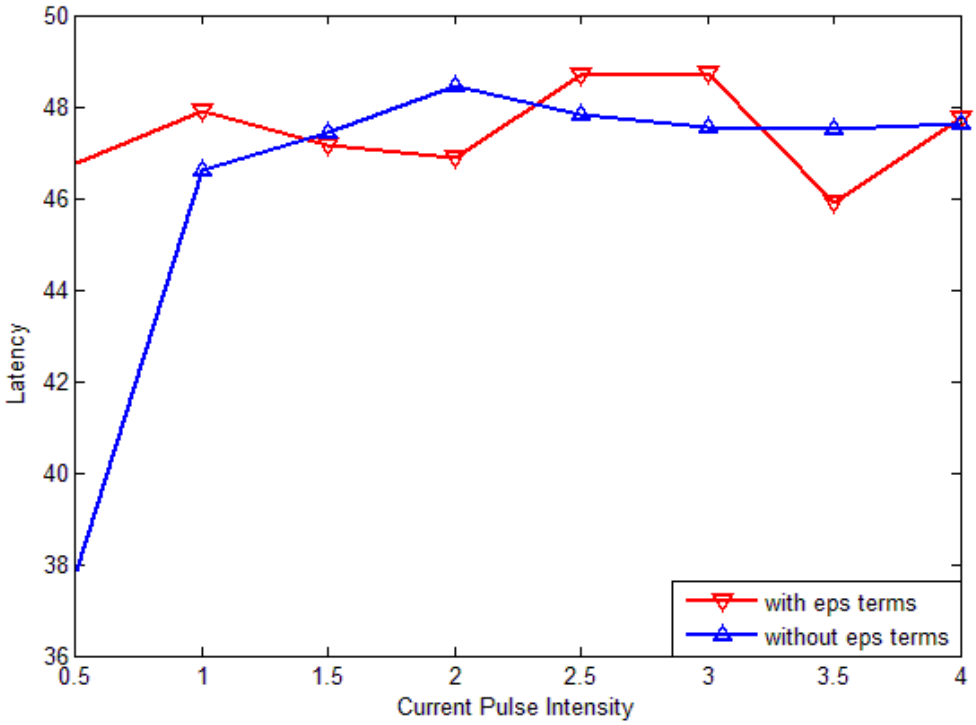

Figure 15: The difference in latency between the two experiments. In the first experiment epsilons value is set to $\varepsilon_m^y = 0.1$, $\varepsilon_u^y = 0.5$, $\varepsilon_m^z = 0.001$, and $\varepsilon_u^z = 0.005$ and the second experiment is set all the epsilons to 0. The intensity is shown in the figure and the I_{base} is set to 2.

In this figure, we got the result as shown above while using the renormalization terms (with eps terms) in the first experiments and second experiments the renormalization terms are set all to zero. We can see the effect of the renormalization in the beginning of the experiments become smaller than the effect in the figure (11, 12, and 13).

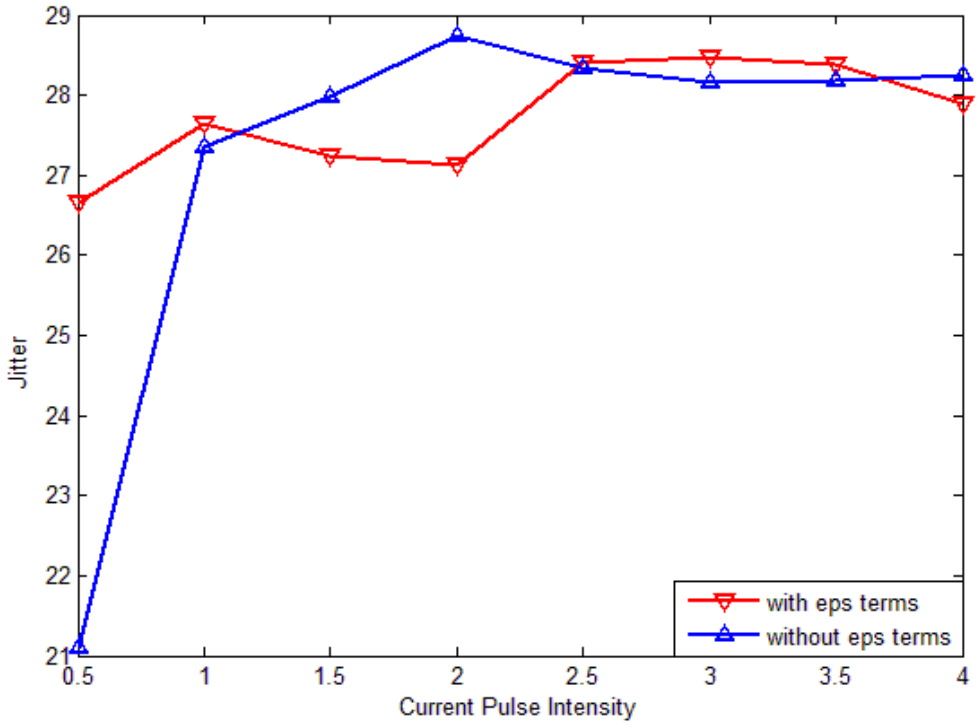

Figure 16: The difference in jitter between the two experiments. In the first experiment epsilons value is set to $\varepsilon_m^y = 0.1, \varepsilon_u^y = 0.5, \varepsilon_m^z = 0.001$, and $\varepsilon_u^z = 0.005$ and the second experiment is set all the epsilons to 0. The intensity is shown in the figure and the I_{base} is set to 2.

In this figure, we got the result as shown above while using the renormalization terms (with eps terms) in the first experiments and second experiments the renormalization terms are set all to zero. We can see the effect of the renormalization in the beginning of the experiments become smaller than the effect in the figure (11, 12, and 13).

Chapter 5

CONCLUSIONS

In this study, the DSM neuron model was investigated from a numerical point of view when exposed to frequent current pulses intensity. The impacts of both the epsilon values and intensity variances on the efficiency, jitter and latency were computed. Correction coefficients were used as an effective measure of renormalization corrections to the model. It should be considered that these renormalization corrections appear from the dilemma of being in doubt of how many open ion-channel numbers there are, even if we know the exact number of open gates.

DSM model neurons appear to be more complex than other models. It shows quicker synchronizing between two DSM neurons (Jibril and Güler 2009), dynamics of the models under constant input currents (Güler 2008) and in addition, its ability in detecting signals under current pulses intensity, that have been inspected during this study, are all the model benefits that deserve tolerating its complexity. Furthermore, it should be taken into consideration that this model is extremely capable of handling the small membrane sizes of the neurons.

It turns out from the numerical experiments that the efficiency ,latency and jitter becomes higher in DSM neuron in which the interaction of current pulse intensity is taken into account .The experiments show also that the epsilon values play an important

role. The absence of the epsilon values makes the neuron in the beginning of the experiment generate spikes in slow manner and after a while the spikes generation will rise in a rapid way as shown in figures (11, 12, 13, 14, 15,and 16), which makes the efficiency ,latency and jitter start to rise until it reaches the steady state when the value of the current pulse intensity equal 2 in the figures(11, 12, 13)and equal 1 in figures(14, 15,16) . The existence of the epsilon values makes the neuron spiking stable, predictable and also makes the neuron more reliable and that will make the efficiency, latency and jitter to reach the steady state from the beginning of the experiments which will enhance the reaction of the neuron and makes it more reliable.

The results reveal that the neurons are extremely able to make a complicated and advantageous use of the channel noise in handling signals. From a technological point of view, the study shows that the DSM model has promising potentialities for signal detection.

REFERENCE

Abbot, D. P. (2002). theorretical Neuroscience Computation and mathematical modeling of neural system. MIT press.

Bezrukov, S. &. (1995). Noise-induced enhancement of signal transduction across voltage-dependent ion channels. Nature, 378, 362–364.

Chow, C. C. (1996). Spontaneous action potentials due to channel fluctuations. Biophysical Journal, 71,3013–3021.

Diba, K. L. (2004). Intrinsic noise in cultured hippocampal neurons: Experiment and modeling. Journal of Neuroscience, 24, 9723–9733.

Nelson E., (1966). Derivation of the Schrödinger Equation from Newtonian Mechanics. Phys. Rev.150, 1079.

Nelson E., (1967). Dynamical Theories of Brownian Motion _Princeton University Press, Princeton,. NJ.

Steur E., (2006). Parameter Estimation in Hindmarsh-Rose Neurons. Traineeship report.

Faisal, A. S. (2008). Noise in the nervous system. nervous system. Nature Reviews Neuroscience, 9, 292–303.

Fox R. F., Y. N. (1994). Emergent collective behavior in large number of globally coupled independently stochastic ion channel. Phys. Rev.3421-3431, 49 .

Güler, M. (2006). Modeling the effects of channel noise in neurons, a study based on disspative stochastic mechanics. Fluct. Noise Lett. 6,L147-L159.

Güler, M. (2007). Dissipative stochastic mechanics for capturing neuronal dynamics under the influence of ion channel noise: Formalism using a special membrane. Physical Review E, 76, 041918(17).

Güler, M. (2008). Detailed numerical investigation of the disspative stochastic mechanics based neuron model. Journal of Computational Neuroscience . 25,211-227.

Güler, M. (2011). Persistent membranous cross correlations due to the multiplicity of gates in ion channels. Journal of Computational Neuroscience ,31,713-724.

Güler, M. (2013). Stochastic Hodgkin-huxley equations with colored noise terms in the conductances. Neural Computation ,25,46-74.

Hodgkin, A. L. (1952). A quantitative description of membrane current and its application to conduction and excitationin in nerve. Journal of Physiology (London Print). 117, 500–544.

Izhikevich, E. M. (2007). Dynamical Systems in Neuroscience:The Geometry of Excitability and Bursting. San Diego, California.

Jacobson, G. A. (2005). Subthreshold voltage noise of rat neocortical pyramidal neurones. Journal of Physiology, 564,145–160.

Jibril, G. &. (2009). The renormalization of neuronal dynamics can enhance temporal synchronization among synaptically coupled neurons. In Proceedings of International Joint Conference on Neural Networks, 1433-1438.

Jung, P. &. (2001). Optimal sizes of ion channel clusters. Europhysics Letters, 56, 29–35.

Kole, M. H. (2006). Single Ih channels in pyramidal neuron dendrites: Properties, distribution, and impact on action potential output. Journal of Neuroscience, 26, 1677–1687.

Rose R. M. and Hindmarsh J. L. (1984). Amodel of Thalamic neuron, Proceedings of the Royal Society of London. Series B, Biological Sciences.

Rubinstein, J. (1995). Threshold fluctuations in an N sodium channel model of the node of Ranvier. Biophysical Journal. 68, 779–785.

Sakmann, B. &. (1995). Single-channel recording (2nded.). New York: Plenum.

Schmid, G. G. (2001). Stochastic resonance as a collective property of ion channel assemblies. Europhysics Letters, 56, 22–28.

Schneidman, E. F. (1998). Ion channel stochasticity may be critical in determining the reliability and precision of spike timing. Neural Computation, 10, 1679–1703.

segev I., J. B. (2003). Cable and compartment models of dendritic trees in bower. The book of genesis 5,55.

Whishaw, K. B. (2012). Fundamentals of Human Physiology Fourth Edition. Virginia United States.